

Spark plasma sintering technique for reaction sintering of $\text{Al}_2\text{O}_3/\text{Ni}$ nanocomposite and its mechanical properties

Toshihiro Isobe^{a,*}, Keiji Daimon^a, Toshihiko Sato^a, Takashi Matsubara^a,
Yasuo Hikichi^a, Toshitaka Ota^b

^a Department of Materials Science and Engineering, Nagoya Institute of Technology, Gokiso, Showa, Nagoya 466-8555, Japan

^b Ceramics Research Laboratory, Nagoya Institute of Technology, 10-6-29 Asahigaoka, Tajimi, Gifu 507-0071, Japan

Received 11 June 2006; received in revised form 21 June 2006; accepted 29 August 2006

Available online 7 November 2006

Abstract

$\text{Al}_2\text{O}_3/\text{Ni}$ nanocomposites were prepared by spark plasma sintering (SPS) using reaction sintering method and the mechanical properties of the obtained nanocomposites are reported. The starting materials of $\text{Al}_2\text{O}_3\text{--NiO}$ solid solution were synthesized from aluminum sulfate and nickel sulfate. These $\text{Al}_2\text{O}_3\text{--NiO}$ powders were changed into Al_2O_3 and Ni phases during sintering process. The obtained nanocomposites showed high relative densities ($>98\%$). SEM micrographs showed homogeneously dispersed Ni grains in the matrix. The 3-point strength and the fracture toughness of the composites significantly improved from 450 MPa in the monolithic $\alpha\text{-Al}_2\text{O}_3$ to 766 MPa in the 10 mol% (2.8 vol.%) Ni nanocomposite and from 3.7 to 5.6 $\text{MPa m}^{1/2}$ in 13 mol% (3.7 vol.%) Ni nanocomposite. On the other hand, Young's modulus and Vickers hardness of the nanocomposites were mostly same as those of the monolithic $\alpha\text{-Al}_2\text{O}_3$.

© 2006 Elsevier Ltd and Techna Group S.r.l. All rights reserved.

Keywords: A. Hot pressing; B. Nanocomposites; C. Mechanical properties; C. Toughness and toughening; D. Al_2O_3 ; D. Spinels; E. Structural applications

1. Introduction

The spark plasma sintering (SPS) is basically a kind of a hot press method, but is developed into a newer technique for sintering the ceramics [1–7]. Fig. 1 shows the schematic model of the SPS apparatus. The main difference of SPS from a hot press is an occurrence of a spark discharge between particles of materials, and the spark discharge accelerates the sintering of material with low grain growth [4–6]. Hence, ceramics prepared by SPS showed high mechanical properties [7]. To discharge the spark plasma, the pulsed dc is applied through the electrodes to top and bottom punches. Carbon sheets are inserted between dies and sample to easily remove the sintered sample from die. Thus, the SPS is carried out inside the carbon sheets and the sintering process carried out in reduction atmosphere. Therefore, SPS is suitable to prepare of ceramics/

metal nanocomposites, which are otherwise generally sintered in inert and/or reduction atmosphere [8–14].

The nanocomposite materials, in which nano-size particles disperse in the matrix, have superior mechanical properties [14,15]. $\text{Al}_2\text{O}_3/\text{Ni}$ nanocomposites are one of the most successful systems. Because the microstructure of these nanocomposites strongly depends on the preparation method, many preparation methods have been attempted [16–22]. The fracture strength of these nanocomposites is significantly enhanced from that of monolithic alumina ceramics.

The in situ reaction sintering method, forming nano-size grains of secondary phase by thermal decomposition of complex compound during reaction sintering, is one of the most appropriate methods to obtain nanocomposites [17]. The starting materials of $\text{Al}_2\text{O}_3\text{--NiO}$ powder synthesized by thermal decomposition of precipitates prepared from aluminum sulfate and nickel sulfate were sintered in a carbon bed at 1500 °C for 1 h after molding. The obtained $\text{Al}_2\text{O}_3/\text{Ni}$ composites have high relative densities and nickel grains (grain size 100–300 nm) dispersed homogeneously in the microstructure. The maximum 3-point bending strength was 408 MPa at 10 mol% Ni sample and the maximum fracture toughness was 9.9 $\text{MPa m}^{1/2}$ at

* Corresponding author. Present address: Advanced Manufacturing Research Institute, National Institute of Advanced Industrial Science and Technology (AIST), 2266-98 Anagahora, Shimo-Shidami, Moriyama-Ku, Nagoya 463-8560, Japan. Tel.: +81 52 736 7378; fax: +81 52 736 7405.

E-mail address: t-isobe@aist.go.jp (T. Isobe).

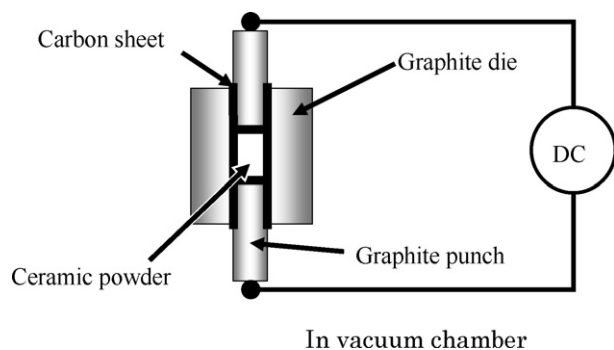


Fig. 1. Schematic model of spark plasma sintering (SPS) apparatus.

40 mol% Ni sample. By homogeneous dispersion of nano-Ni grains, the obtained composites showed the maximum 3-point bending strength at much lower Ni content than previously reported nickel content. Thus, $\text{Al}_2\text{O}_3/\text{Ni}$ nanocomposites were prepared by the in situ reaction sintering method in carbon atmosphere. This method is also preferable to SPS which is carried out in carbon atmosphere, and it is expected that the mechanical properties of the nanocomposites are further enhanced by in situ sintering method using SPS system.

In this study, the $\text{Al}_2\text{O}_3/\text{Ni}$ nanocomposites were prepared by SPS using $\text{Al}_2\text{O}_3\text{--NiO}$ solid solution as raw material and mechanical properties of the obtained composites were evaluated.

2. Experimental procedure

2.1. Preparation of composites

$\text{Al}_2\text{O}_3\text{--NiO}$ co-precipitated powders were prepared by the water solution heating method [17,23]. High purity aluminum sulfate ($\text{Al}_2(\text{SO}_4)_3 \cdot 14\text{--}18\text{H}_2\text{O}$, Hayashi Pure Chemical Ind., Japan) and high purity nickel sulfate ($\text{NiSO}_4 \cdot 6\text{H}_2\text{O}$, Kishida Chemical Co., Japan) (0–13 mol%) were dissolved and mixed in water for 2 h. The obtained solution was rapidly dried by microwave (MR-P1510, Hitachi, Japan), calcined at 900 °C for 4 h to remove sulfate and further calcined at 1250 °C for 1 h. The obtained powder was wet ball milled in an ethanol for 48 h and dried at 110 °C for 2 h.

The obtained powders were sintered by SPS apparatus (SPS-515S, Sumitomo Coal Mining, Japan). The dimension of the carbon die barrel and inner aperture was 40 and 20 mm ϕ , respectively. To ensure the good electrical contact and reduce the co-precipitated powder, carbon sheets were inserted between the punches and die (Fig. 1). The carbon die was covered with ceramic wool for thermal insulation and the co-precipitated powder was packed in the die. Sintering conditions were at 1350 °C for 6 min (heating rate: 100 °C/min) and a pressure of 20 MPa applied from the beginning of the sintering. The temperature of the die was measured with an optical pyrometer which was focused to the die surface.

2.2. Characterization

The phase composition was identified by X-ray diffractometry (XRD) using Cu K α radiation (RAD-B, Rigaku, Japan).

The relative density of the specimens was measured by the Archimedes technique using water. The microstructure of the surface was observed using a scanning electron microscope (SEM) (JSM-5200, JEOL, Japan). Young's modulus was measured using an ultrasonic method using a sintered specimen with diameter of 20 mm ϕ and thickness of 10 mm. The sintered specimens were cut by a diamond wheel to the dimension of 2 mm \times 2 mm \times 10 mm, and the specimen surfaces were polished with 3 and 6 μm diamond pastes. Fracture strength measurements were carried out by a 3-point bending test with a span length of 8 mm and crosshead speed of 0.5 mm/min (AGS-5kND, Shimadzu, Japan). The average bending strength was obtained from measurements of 10 samples. Vickers hardness test was performed on micro-Vickers hardness tester (AVK-A, Akashi, Japan) on the polished surface. Fracture toughness were estimated by indentation fracture (IF) method, which was calculated from the following equation:

$$K_{\text{Ic}} = 0.026 \frac{E^{0.5}(P)^{0.5}a}{C^{1.5}}$$

where E is the Young's modulus, P the load applied for indentation, a the dimension of indentation and C is the crack length measured from the center of contact pattern.

3. Results and discussion

3.1. Phase change during sintering

Fig. 2 shows the XRD patterns of the obtained $\text{Al}_2\text{O}_3\text{--NiO}$ powders before sintering. The powder without Ni shows only $\alpha\text{--Al}_2\text{O}_3$

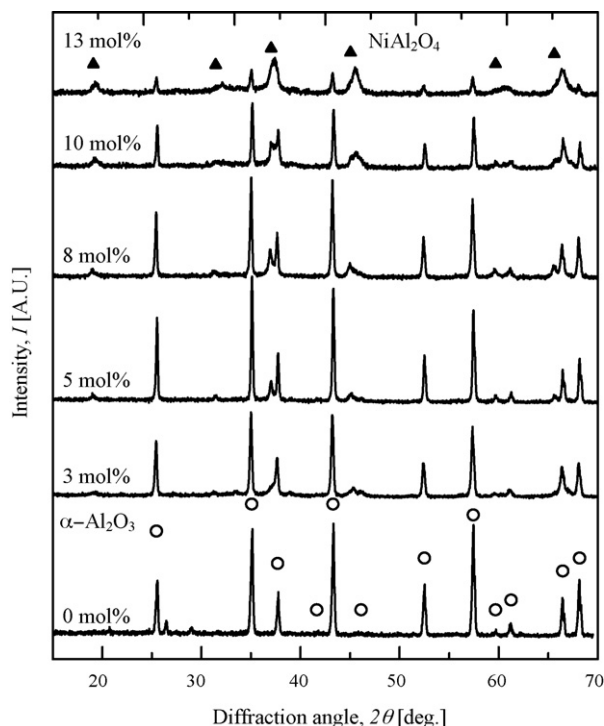


Fig. 2. XRD pattern of $\text{Al}_2\text{O}_3\text{--Ni}$ solid solution powders after calcining at 1250 °C for 1 h.

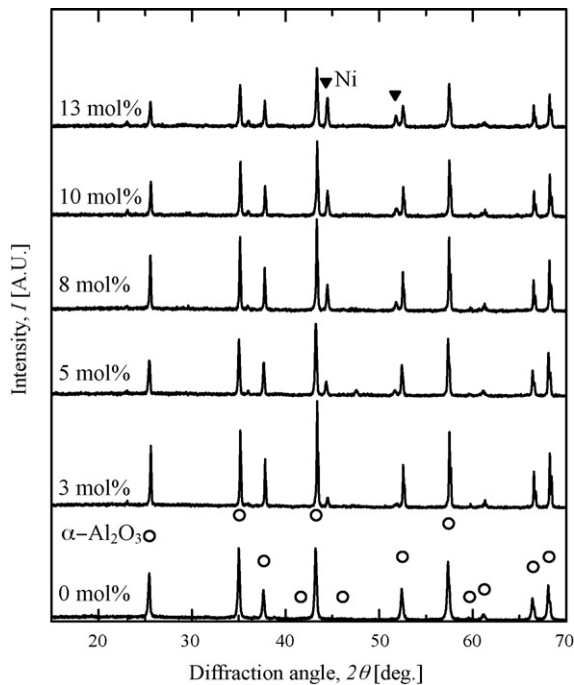


Fig. 3. XRD pattern of $\text{Al}_2\text{O}_3/\text{Ni}$ composites after sintering at 1350°C for 6 min.

Al_2O_3 peaks and the powders containing Ni show peaks assigned to $\alpha\text{-Al}_2\text{O}_3$ and NiAl_2O_4 spinel. The powder for in situ reaction sintering ideally consists of the mono phase to avoid the problem of density difference between ceramics phase and secondary metal during mixing process. The obtained powders consisted of two phases but the densities of $\alpha\text{-Al}_2\text{O}_3$ (4.0 g/cm^3) and NiAl_2O_4 (4.4 g/cm^3) are similar, which is fair for the raw material for in situ reaction sintering. Fig. 3 shows the XRD patterns of the composites obtained by SPS at 1350°C for 6 min. These XRD patterns show that all the samples consisted of only $\alpha\text{-Al}_2\text{O}_3$ and Ni phases. This is because of the phase changes from NiAl_2O_4 to $\alpha\text{-Al}_2\text{O}_3$ and Ni as reported in the previous study [17,23].

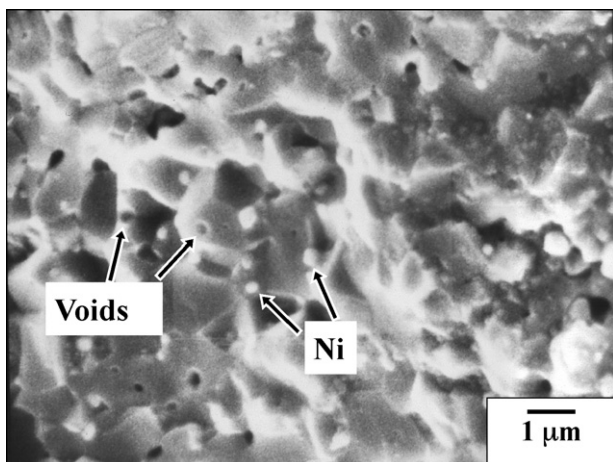


Fig. 4. SEM micrograph of $\text{Al}_2\text{O}_3/10\text{ mol\% Ni}$ composite.

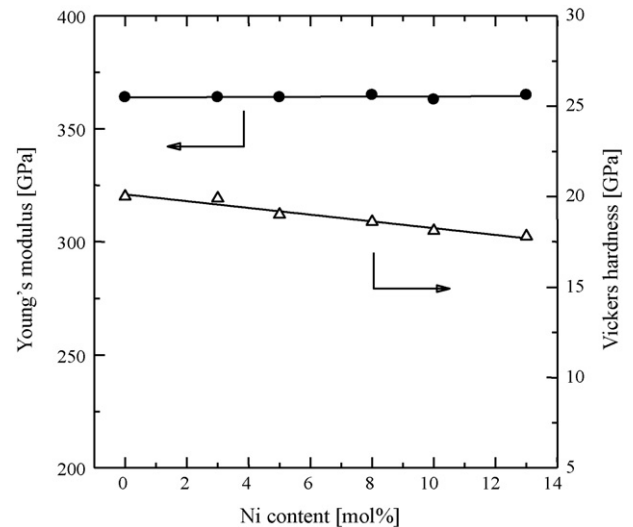


Fig. 5. Young's modulus and Vickers hardness of $\text{Al}_2\text{O}_3/\text{Ni}$ composites as a function of Ni content.

3.2. Microstructure and relative density

Fig. 4 shows the fracture surface of the 10 mol% Ni composites. The microstructures of all samples show homogeneous dispersion of Ni grains in the alumina matrix. These Ni grains were originated from NiAl_2O_4 spinel. SEM micrograph also showed many voids, which were formed by Ni grains peeled off from alumina matrix. It is considered that these voids indicate that the Ni grains influence the fracture of the ceramics and improvement of the fracture toughness. The relative densities of the composites measured by Archimedes technique were $>98\%$ of the theoretical densities.

3.3. Mechanical properties

Fig. 5 shows Young's modulus (E) and Vickers micro hardness (H_V) of the resulting $\text{Al}_2\text{O}_3/\text{Ni}$ composites. The E and

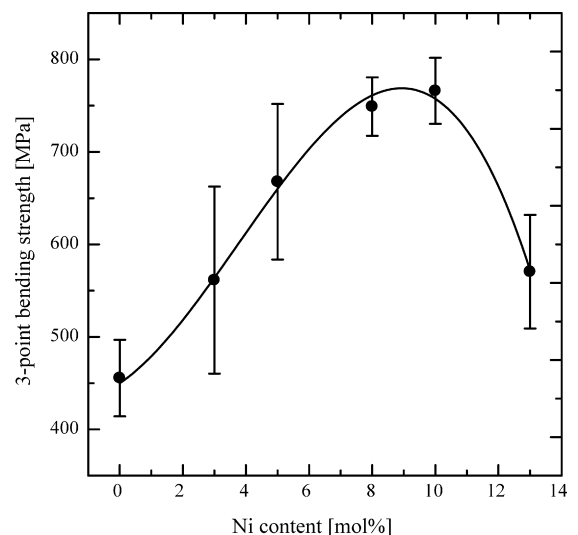


Fig. 6. Relationship between nickel content and 3-point bending strength of $\text{Al}_2\text{O}_3/\text{Ni}$ composites.

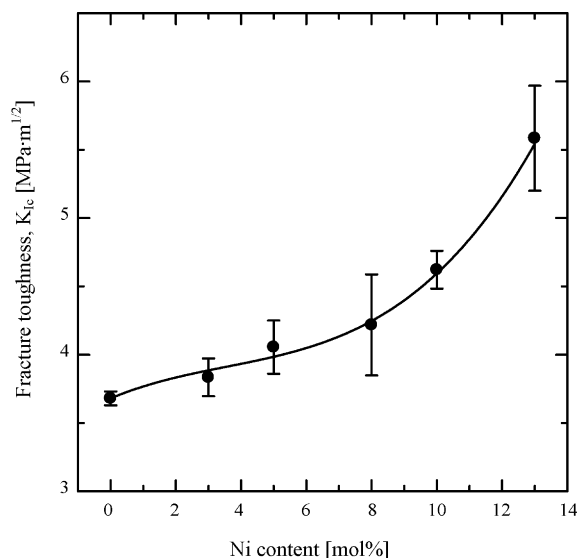


Fig. 7. Relationship between nickel content and fracture toughness of $\text{Al}_2\text{O}_3/\text{Ni}$ composites.

H_V values of monolithic $\alpha\text{-Al}_2\text{O}_3$ are 364 and 20.0 GPa, respectively. The E -values were nearly same with increase in Ni content and H_V of the resulting $\text{Al}_2\text{O}_3/\text{Ni}$ composites were slightly decreased with increase in Ni content. It is considered that the little decrease of these values were due to Ni addition. Nevertheless, these values of the composites were similar to monolithic $\alpha\text{-Al}_2\text{O}_3$ because of a very low Ni content (13 mol% = 3.7 vol.%).

On the other hand, the 3-point bending strength and fracture toughness showed a large increase with such a low Ni content. Fig. 6 shows the change of 3-point bending strength (σ) as a function of Ni content in the composites. The σ -value increases up to 766 MPa (Weibull modulus of 21.9) by dispersing 10 mol% Ni, which is only 2.8 vol.%. However, the strength decreases with increasing Ni content beyond 10 mol%. The maximum strength of the composites is generally obtained by mixing 5–10 vol.% of the second phase, however the composites prepared by in situ reaction sintering method show the maximum strength at only 2–3 vol.% [17]. The maximum strength of the present sample was also obtained at 2.8 vol.%. This is owing to homogeneous dispersion of nano-Ni grains in alumina matrix.

The relationship between Ni content and the fracture toughness (K_{Ic}) of the obtained composites is shown in Fig. 7. The K_{Ic} values of monolithic $\alpha\text{-Al}_2\text{O}_3$ was 3.7 MPa m^{1/2}. This value increased with increase in Ni content and reached up to 5.6 MPa m^{1/2} at 13 mol% Ni content. The mechanism of the toughening is thought to be frontal zone toughening and crack bridging, which is the general toughening mechanism of the nano-composites [14,15].

To compare the improvements of the mechanical properties the mechanical properties of the present composites, monolithic $\alpha\text{-Al}_2\text{O}_3$ [24] and $\text{Al}_2\text{O}_3/\text{Ni}$ composites prepared by in situ reaction sintering method (previous study) [17], pressureless sintering method [18,19], hot press method [20,21] and SPS method [13,14] are listed in Table 1. The fracture strength and fracture toughness of the present composites showed relatively higher values than the reported values. To evaluate the effect of the nickel addition, Tuan et al. have used the ratio of the mechanical properties of composite to that of matrix [16]. Comparison of the ratios is appropriate to the evaluation of the mechanical properties, because each report uses the different condition to measure these properties. The ratio of the fracture strengths (σ/σ_0) and fracture toughness (K_{Ic}/K_{Ic0}) were also listed in Table 1. The present material is stronger than the other reported materials when compared with their σ/σ_0 and K_{Ic}/K_{Ic0} values. These excellent mechanical properties are due to homogeneously dispersed small Ni grains in alumina matrix obtained by this new method hence demonstrate the usefulness of this new preparation technique for nanocomposites.

4. Summary

$\text{Al}_2\text{O}_3/\text{Ni}$ nanocomposites were prepared by SPS using $\text{Al}_2\text{O}_3\text{-NiO}$ solid solution as raw material and mechanical properties of the obtained nanocomposites were reported. Starting powders ($\text{Al}_2\text{O}_3\text{-NiO}$ powders) were changed into Al_2O_3 and Ni phases during sintering process. The relative densities of the obtained $\text{Al}_2\text{O}_3/\text{Ni}$ nanocomposites were >98%. Ni grains were homogeneously dispersed in the microstructure. Young's modulus and Vickers hardness of the nanocomposites were similar to those of the monolithic $\alpha\text{-Al}_2\text{O}_3$. By contrast, the 3-point strength of the composites increased from 450 MPa in the monolithic $\alpha\text{-Al}_2\text{O}_3$ to 766 MPa in the 10 mol% (2.8 vol.%) Ni nanocomposite. The fracture

Table 1
Comparison of mechanical properties of the $\text{Al}_2\text{O}_3/\text{Ni}$ composites prepared by various methods

	Ni content (vol.%)	R.D. ^a (%)	σ (MPa)	K_{Ic} (MPa m ^{1/2})	σ/σ_0	K_{Ic}/K_{Ic0}
This study	2.8	>98	766	4.6	1.70	1.25
Previous study [17]	2.8	95	408	5.8	1.15	2.20
Pressureless [18]	5	97	526	4.2	1.07	1.17
Pressureless [19]	7.6	90	439		1.28	
Hot press [20]	5	>98	1090	3.5	1.56	1.00
Hot press [21]	5.5	>98	500	4.1	1.43	1.18
SPS [12]	3	>98	984	4.5	1.64	1.05
SPS [13]	5	>98	650	3.2	0.90	0.94
$\alpha\text{-Al}_2\text{O}_3$ [24]	0	>98	380	3.5		

^a Relative density.

toughness of the nanocomposites were enhanced from 3.7 to 5.6 MPa m^{1/2} with increasing Ni content. The σ/σ_0 and K_{Ic}/K_{Ic0} values of the present samples were higher than previously reported values. Therefore, the new SPS technique, which is a reaction sintering technique using SPS apparatus, is successfully demonstrated for the preparation of Al₂O₃/Ni nanocomposite.

Acknowledgement

The authors thank Dr. C.D. Madhusoodana of Tokyo Institute of Technology for critical reading and editing of this manuscript.

References

- [1] M. Tokita, Trends in advanced SPS spark plasma sintering system and technology, *J. Soc. Powder Technol., Japan* 30 (11) (1993) 790–804.
- [2] M. Otori, Sintering, consolidation, reaction and crystal growth by the spark plasma system (SPS), *Mater. Sci. Eng. A* 287 (2) (2000) 183–188.
- [3] G.D. Zhan, J.D. Kuntz, J. Wan, A.K. Mukherjee, Single-wall carbon nanotubes as attractive toughening agents in alumina-based nanocomposites, *Nat. Mater.* 2 (1) (2003) 38–42.
- [4] S.W. Wang, L.D. Chen, T. Hirai, Densification of Al₂O₃ powder using spark plasma sintering, *J. Mater. Res.* 15 (4) (2000) 982–987.
- [5] Z. Shen, M. Johnsson, Z. Zhao, M. Nygren, Spark plasma sintering of alumina, *J. Am. Ceram. Soc.* 85 (8) (2002) 1921–1927.
- [6] T. Takeuchi, M. Tabuchi, H. Kageyama, Y. Suyama, Preparation of dense BaTiO₃ ceramics with submicrometer grains by spark plasma sintering, *J. Am. Ceram. Soc.* 82 (4) (1999) 939–943.
- [7] L. Gao, J.S. Hong, H. Miyamoto, S.D.D.L. Torre, Bending strength and microstructure of Al₂O₃ ceramics, densified by spark plasma sintering, *J. Eur. Ceram. Soc.* 20 (12) (2000) 2149–2152.
- [8] X. Yao, Z. Huang, L. Chen, D. Jiang, S. Tan, D. Michel, G. Wang, L. Mazerolles, J.L. Pastol, Alumina–nickel composites densified by spark plasma sintering, *Mater. Lett.* 59 (18) (2005) 2314–2318.
- [9] D.D. Jayaseelan, R. Sivakumar, T. Nishikawa, S. Honda, H. Awaji, Mullite-molybdenum composites fabricated by pulse electric current sintering technique, *J. Eur. Ceram. Soc.* 22 (5) (2002) 761–768.
- [10] R. Sivakumar, D.D. Jayaseelan, T. Nishikawa, S. Honda, H. Awaji, Influence of MgO on microstructure and properties of mullite-Mo composites fabricated by pulse electric current sintering, *Ceram. Int.* 27 (5) (2001) 537–541.
- [11] K.H. Min, S.T. Oh, Y.D. Kim, I.H. Moon, Processing and fracture toughness of nano-sized Cu-dispersed Al₂O₃ composites, *J. Alloys Compd.* 352 (1–2) (2003) 163–167.
- [12] U. Leela-Adisorn, T. Matsunaga, Y. Kobayashi, S.M. Choi, H. Awaji, Soaking method for fabrication of alumina-based nanocomposites, *Ceram. Int.* 31 (6) (2005) 803–809.
- [13] B.S. Kim, T. Sekino, T. Nakayama, M. Wada, J.S. Lee, K. Niihara, Pulse electric current sintering of alumina/nickel nanocomposites, *Mater. Res. Innov.* 7 (2) (2003) 57–61.
- [14] S.M. Choi, H. Awaji, Nanocomposites—a new material design concept, *Sci. Technol. Adv. Mater.* 6 (1) (2005) 2–10.
- [15] K. Niihara, New design concept of structural ceramic/ceramic nanocomposites, *J. Ceram. Soc. Jpn.* 99 (10) (1991) 974–982.
- [16] W.H. Tuan, R.J. Brook, Processing of alumina/nickel composites, *J. Eur. Ceram. Soc.* 10 (2) (1992) 95–100.
- [17] T. Isobe, K. Daimon, K. Ito, T. Matsubara, Y. Hikichi, T. Ota, Preparation and properties of Al₂O₃/Ni composite from NiAl₂O₄ spinel by in-situ reaction sintering method, *Ceram. Int.* 33 (2007) 1211–1215.
- [18] R.Z. Chen, W.H. Tuan, Pressureless sintering of Al₂O₃/Ni nanocomposites, *J. Eur. Ceram. Soc.* 19 (4) (1999) 463–468.
- [19] M. Lieberthal, W.D. Kaplan, Processing and properties of Al₂O₃ nanocomposites reinforced with sub-micron Ni and NiAl₂O₄, *Mater. Sci. Eng. A* 302 (1) (2001) 83–91.
- [20] T. Sekino, T. Nakajima, S. Ueda, K. Niihara, Reduction and sintering of a nickel-dispersed-alumina composite and its properties, *J. Am. Ceram. Soc.* 80 (5) (1997) 1139–1148.
- [21] J. Lu, L. Gao, J. Sun, L. Gui, L. Guo, Effect of nickel content on the sintering behavior, mechanical and dielectric properties of Al₂O₃/Ni composites from coated powders, *Mater. Sci. Eng. A* 293 (1) (2000) 223–228.
- [22] G.J. Li, X.X. Huang, K.J. Guo, Fabrication and mechanical properties of Al₂O₃/Ni composite from two different powder mixtures, *Mater. Sci. Eng. A* 352 (1) (2003) 23–28.
- [23] K. Daimon, T. Isobe, Y. Hikichi, T. Ota, Partial reduction of reactive NiAl₂O₄ spinel prepared from a sulfate solid solution, *Nippon Kagaku Kaishi* 2002 (2) (2002) 195–199.
- [24] R.G. Munro, Evaluated material properties for a sintered α -alumina, *J. Am. Ceram. Soc.* 80 (8) (1997) 1919–1928.